Molecular Cell
Article

Oxidative Protein Folding by an Endoplasmic Reticulum-Localized Peroxiredoxin

Ester Zito,[1] Eduardo Pinho Melo,[1,5] Yun Yang,[1] Åsa Wahlander,[1] Thomas A. Neubert,[1,4] and David Ron[1,2,3,6,*]
[1]Kimmel Center for Biology and Medicine at the Skirball Institute
[2]Department of Cell Biology
[3]Department of Medicine
[4]Department of Pharmacology
New York University School of Medicine, New York, NY 10016, USA
[5]Institute for Biotechnology and Bioengineering, Centre for Molecular and Structural Biomedicine, Universidade do Algarve, Portugal
[6]Institute of Metabolic Sciences, University of Cambridge, Cambridge CB2 0QQ, UK
*Correspondence: dr360@medschl.cam.ac.uk
DOI 10.1016/j.molcel.2010.11.010

SUMMARY

Endoplasmic reticulum (ER) oxidation 1 (*ERO1*) transfers disulfides to protein disulfide isomerase (PDI) and is essential for oxidative protein folding in simple eukaryotes such as yeast and worms. Surprisingly, ERO1-deficient mammalian cells exhibit only a modest delay in disulfide bond formation. To identify ERO1-independent pathways to disulfide bond formation, we purified PDI oxidants with a trapping mutant of PDI. Peroxiredoxin IV (PRDX4) stood out in this list, as the related cytosolic peroxiredoxins are known to form disulfides in the presence of hydroperoxides. Mouse embryo fibroblasts lacking ERO1 were intolerant of PRDX4 knockdown. Introduction of wild-type mammalian PRDX4 into the ER rescued the temperature-sensitive phenotype of an *ero1* yeast mutation. In the presence of an H_2O_2-generating system, purified PRDX4 oxidized PDI and reconstituted oxidative folding of RNase A. These observations implicate ER-localized PRDX4 in a previously unanticipated, parallel, ERO1-independent pathway that couples hydroperoxide production to oxidative protein folding in mammalian cells.

INTRODUCTION

Disulfide bond formation in the endoplasmic reticulum involves the transfer of electrons from the reduced cysteines of unfolded proteins to oxidoreductases of the protein disulfide isomerase (PDI) family. This catalytic cycle is completed by the reoxidation of the reduced PDIs. Genetic studies in yeast and biochemical analysis in vitro have implicated the lumenal oxidase ERO1 in PDI reoxidation and disulfide bond formation (reviewed in Tu and Weissman, 2004; Sevier and Kaiser, 2008).

Yeast lacking ERO1 are nonviable, indicating that ERO1 is required for the essential process of disulfide bond formation (Frand and Kaiser, 1998; Pollard et al., 1998). Mammals have two genes encoding proteins homologous to yeast ERO1, known as ERO1α (or *ERO1L*) (Cabibbo et al., 2000) and ERO1β (or *ERO1Lb*) (Pagani et al., 2000). Biochemical studies in vitro and ability to complement the yeast mutation in vivo prove that the mammalian proteins also function as ER oxidases, accepting electrons from reduced PDI (Cabibbo et al., 2000; Mezghrani et al., 2001; Appenzeller-Herzog et al., 2008; Baker et al., 2008; Blais et al., 2010).

The two isoforms have different tissue distribution: ERO1α is broadly expressed, whereas ERO1β expression is greatly enriched in the endocrine pancreas and in immunoglobulin-secreting cells (Pagani et al., 2000; Dias-Gunasekara et al., 2005; Zito et al., 2010). Compromise of ERO1β expression in mice delays oxidative folding of proinsulin (Zito et al., 2010). Surprisingly, compounding the loss of ERO1β by loss of ERO1α does not exacerbate the mild diabetic phenotype or the impaired insulin secretion of the single ERO1β mutant (Zito et al., 2010). Given the critical role of disulfide bond formation in insulin biogenesis (Liu et al., 2007), this observation suggests the existence of pathways to mammalian ER oxidation that function in parallel to ERO1. Fly genetics also provides evidence for the existence of such parallel pathways. While the single ERO1 gene in that species (known as *kiga*) is essential to animal development, clones of homozygous mutant *kiga* cells are presumably capable of oxidative protein folding, as they expand normally in the wing disc and pupal notum (Tien et al., 2008).

Various processes emerge as candidates for ERO1-independent disulfide bond formation. Early studies had emphasized the potential for selective import of disulfide-bonded glutathione into the ER as a driver of protein oxidation (Hwang et al., 1992). More recently Ruddock and colleagues have called attention to the potential role of direct oxidation of cysteine residues by H_2O_2 or dehydroascorbate as mechanisms for disulfide bond formation (Karala et al., 2009; Saaranen et al., 2010). The secreted enzymes, QSOX1 and QSOX2, can catalyze the oxidation of cysteines on unfolded proteins, and an ER-localized fraction of QSOX could play a role in ER oxidation (Kodali and Thorpe, 2010). Finally, the vitamin K epoxide reductase can utilize oxidized vitamin K to drive PDI oxidation and thereby promote disulfide bond formation (Li et al., 2010).

Here we report on the application of an unbiased method for uncovering candidates in the parallel ERO1-independent

pathway to protein oxidation and in the experimental indictment of the ER-localized peroxiredoxin IV (PRDX4) in that pathway.

RESULTS

PRDX4 Forms Stable Complexes with an Active-Site Trapping Mutant of PDI

The minimal effect of ERO1 loss of function on disulfide bond formation in higher eukaryotes was previously inferred from indirect measurements (Tien et al., 2008; Zito et al., 2010). To assess this process directly we monitored the disulfide bond-dependent changes in mobility on nonreducing sodium dodecyl sulfate polyacrylamide gel electrophoresis (SDS-PAGE) as newly synthesized immunoglobulin M (IgM) monomers progress to dimers and decamers in pulse-chase-labeled lipopolysaccharide-induced blasts cultured from the spleens of wild-type or compound *Ero1L;Ero1Lb* mutant mice (lacking ERO1α and ERO1β protein). The rate of progression is nearly indistinguishable in the two genotypes (Figure 1A), confirming the existence of parallel pathways for disulfide bond formation in the ER of ERO1-deficient cells.

ERO1 accepts electrons directly from the reduced C-terminal active site of PDI (Tsai and Rapoport, 2002; Wang et al., 2009). We reasoned that if a parallel pathway were to exploit a similar step in electron transfer, the acceptor protein (the oxidant of PDI) could be trapped in complex with a mutant PDI that is missing the resolving cysteine of its C-terminal active site. To establish this system, we expressed wild-type-, single (C400S)-, and double (C56S; C400S)-trapping mutant FLAG-M1 epitope-tagged human PDI proteins by transient transfection of HEK293T cells. Cell lysates were prepared in the presence of N-Ethylmaleimide (NEM) to quench free thiols, and protein complexes were immunopurified by the FLAG-M1 tag. Immunoblot of a reducing gel showed that the C-terminal trapping mutant PDI^{C400S} associated with more ERO1α than the wild-type or the double-mutant $PDI^{C56S,C400S}$ (Figure 1B, upper panel). Immunoblot of the nonreducing gel showed that all the detectable ERO1α that copurified with PDI^{C400S} was associated in a high-molecular-disulfide-bonded complex (Figure 1B, lower panel). A species of similar mobility was also detected with the anti-FLAG antibody (Figure 1B, lower panel). These observations confirmed the utility of the trapping mutant PDI^{C400S} in stably associating with a known ER oxidase.

To identify other proteins that may associate with the trapping mutant PDI^{C400S} in a disulfide-bonded complex, we excised the region of the nonreducing SDS-PAGE containing the trapped complexes. After in-gel reduction, alkylation, and digestion with trypsin, the peptides eluted from the gel slices were analyzed by liquid chromatography (LC-MS/MS) (Figure 2A). The corresponding human proteins were sorted based on their exponentially modified protein abundance index (emPAI) (Figure 2B).

Among the high emPAI scoring proteins discovered in complex with PDI, PRDX4 seemed the most likely to play a role in ER oxidation: like other members of the family of 2-cysteine peroxiredoxins, PRDX4 has been reported to reduce H_2O_2 to water by forming an intersubunit disulfide bond (Hall et al., 2009; Ikeda et al., 2010; Tavender and Bulleid, 2010).

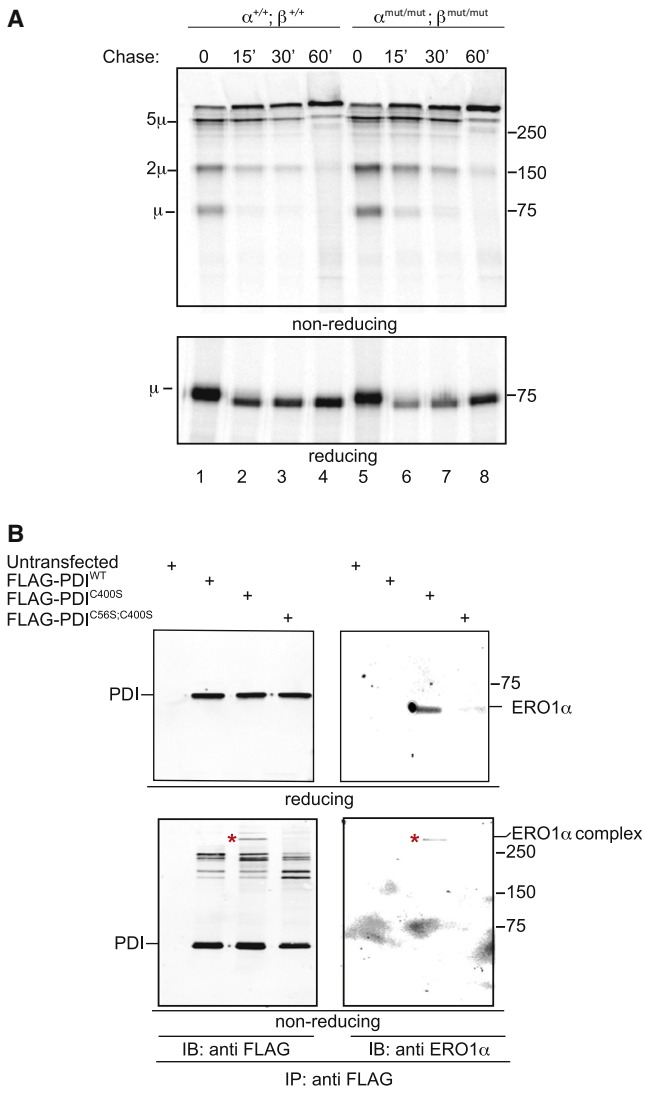

Figure 1. A Trapping Mutant of PDI Engages the Known Downstream Electron Acceptor, ERO1α, in Mammalian Cells

(A) Autoradiograph of IgM from metabolically labeled wild-type ($\alpha^{+/+};\beta^{+/+}$) and ERO1 mutant ($\alpha^{mut/mut};\beta^{mut/mut}$) lipopolysaccharide blasts. Cells were labeled with [^{35}S]methionine-cysteine for 15 min and chased for the indicated time with unlabeled media before lysis and immunoprecipitation. The upper panel is a radiograph of a nonreducing gel and the lower panel is a reducing gel. The migration of IgM monomers (μ), dimers (2μ), and pentamers of dimers (5μ) is indicated.

(B) Immunoblots of FLAG-tagged proteins (left) or endogenous ERO1α (right) immunopurified with the FLAG-M1 antibody from lysates of HEK293T cells that were untransfected or transfected with expression plasmids of the indicated proteins. The upper panels are of reducing and the lower panels are of nonreducing gels. The low-mobility complex containing ERO1α–immunoreactive material in complex with the FLAG-tagged PDI C-terminal active-site trapping mutant ($FLAG\text{-}PDI^{C400S}$) is noted by an asterisk on both nonreducing gels.

Importantly, PRDX4 has been shown to reside in the ER lumen as a soluble protein (Tavender et al., 2008).

Substantial amounts of endogenous PRDX4 immunoreactivity were recovered in complex with the tagged trapping mutant

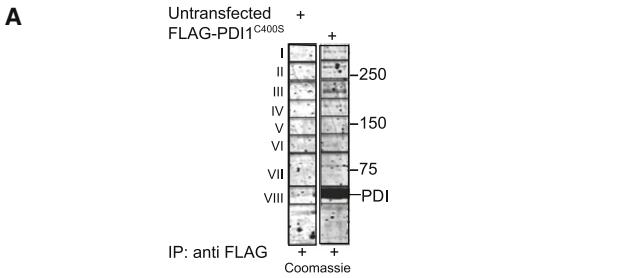

B

IPI	Protein	emPAI
IPI00010796	P4HB Protein disulfide-isomerase	4.09
IPI00003362	HSPA5 (BiP)	1.03
IPI00011937	**PRDX4 (Peroxiredoxin-4)**	**0.36**
IPI00027230	HSP90B1 (Grp94)	0.23
IPI00386755	ERO1L (ERO1alpha)	0.19
IPI00019912	HSD17B4 (Peroxisomal multifunctional enzyme type 2)	0.13
IPI00006482	ATP1A1 (Sodium/potassium-transporting ATPase subunit alpha-1)	0.12
IPI00219077	LTA4H (Isoform 1 of Leukotriene A-4 hydrolase)	0.1
IPI00429633	ERO1LB (ERO1beta)	0.06
IPI00011454	GANAB (Isoform 2 of Neutral alpha-glucosidase AB)	0.06
IPI00303207	ABCE1 (ATP-binding cassette sub-family E member 1)	0.05
IPI00291136	COL6A1 (Collagen alpha-1(VI) chain)	0.03
IPI00000877	HYOU1 (Hypoxia up-regulated protein 1 - ORP150)	0.03

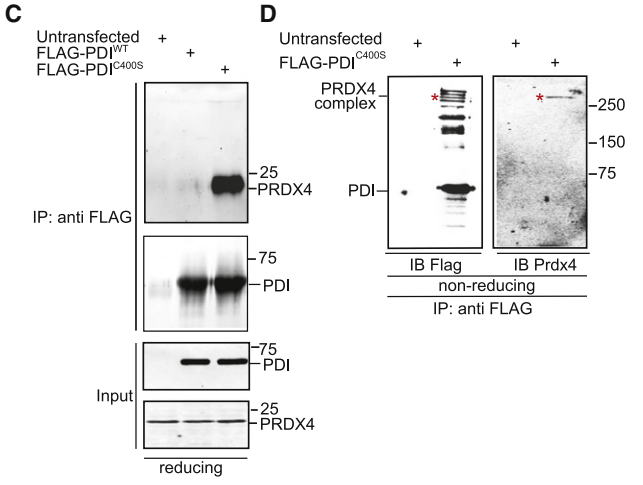

Figure 2. A PDI Active-Site Trapping Mutant Engages PRDX4 in Mammalian Cells

(A) Coomassie-stained nonreducing SDS-PAGE of proteins immunopurified in complex with FLAG-tagged PDI trapping mutant from untransfected and transfected cells. The boxes demarcate the binning for the mass spectrometric protein analysis.

(B) List of proteins identified by LC-MS/MS sequencing of tryptic peptides of endogenous proteins captured in a disulfide-linked complex by a FLAG-M1-tagged trapping mutant PDI^{C400S} expressed in HEK293T cells (shown in A). Known cytosolic, nuclear, and mitochondrial proteins were removed from the list and the remaining proteins were sorted by descending exponentially modified protein abundance index (emPAI) (Ishihama et al., 2005). The proteins are identified by their International Protein Index accession number (IPI) and their common name.

(C) Immunoblot of endogenous PRDX4 and FLAG-tagged wild-type PDI and trapping mutant PDI^{C400S} immunopurified with the FLAG-M1 antibody from lysates of HEK293T cells that were untransfected or transfected with expression plasmids for the indicated proteins. The lower two panels are of the same proteins in the lysates before the IP ("Input"). The proteins shown were resolved on reducing SDS-PAGE.

(D) FLAG and endogenous PRDX4 immunoblot of a nonreducing gel with samples as in (B). The low-mobility complex containing PRDX4 immunoreactive material in complex with FLAG-PDI^{C400S} is noted by an asterisk on both nonreducing gels.

PDI^{C400S} in HEK293T cells (Figure 2C). On nonreducing gels the complex migrated slowly, consistent with disulfide bonding (Figure 2D). The FLAG-M1 epitope of the tagged PDI^{C400S} is exposed only after cleavage of the protrypsinogen signal sequence by the ER-localized leader sequence peptidase (Brizzard et al., 1994); thus the trapping of endogenous PRDX4 probably reflects an interaction that took place in the lumen of the ER. Based on these hints, we hypothesized that PRDX4 may utilize lumenal H_2O_2 to form disulfides that it then passes on to PDI to oxidize ER client proteins.

PRDX4 Buffers the Consequences of ERO1 Deficiency in Mammalian Cells

PRDX4 is not an essential ER enzyme, as mice with a deletion of the first exon, encoding the signal sequence, are viable and fertile (Iuchi et al., 2009). However, we considered that if PRDX4 contributed significantly to disulfide bond formation, its function might become essential in cells lacking ERO1. Therefore, we compared the effect of PRDX4 knockdown on survival and growth of mouse embryo fibroblasts derived from wild-type and *Ero1L;Ero1Lb* mutant mice.

Lentiviral vectors carrying a dominant selection marker imparting puromycin resistance were used to transduce small hairpin RNAs targeting mouse PRDX4. In both wild-type and double-mutant cells, transduction led to marked decline in endogenous PRDX4 signal (Figure 3A). In the ERO1 wild-type background, selection with puromycin resulted in a thick growth of PRDX4 knockdown cells, consistent with the mild phenotype of the PRDX4 mutation in mice. However, transduction of the shRNA to PRDX4 elicited growth of fewer puromycin-resistant colonies of *Ero1L;Ero1Lb* double-mutant mouse embryonic fibroblasts (MEFs), indicating that cells lacking ERO1 require PRDX4 for normal growth (Figures 3B and 3C).

Cellular ultrastructure was impaired by PRDX4 shRNA. The mild ER dilation noted basally in the *Ero1L;Ero1Lb* double-mutant MEFs was conspicuously enhanced by further compromise of PRDX4 expression (Figure 3D). Together, these observations indicate that PRDX4 has an important role in cells lacking ERO1 and suggest that this essential role is involved in ER homeostasis.

To further characterize the impact of PRDX4 loss in MEFs lacking *ERO1*, we examined their sensitivity to exogenously added dithiothreitol (DTT), a disulfide-bond-reducing agent. Cells were exposed to a brief 30 min pulse of 5 mM DTT followed by washout with fresh media. The cell mass quantified 3 hr later was markedly lower in the ERO1 mutant cells compounded by PRDX4 knockdown (Figure 4A).

ERO1-deficient cells had baseline impairment in collagen secretion (another reflection of ERO1's importance to mammalian physiology) that was further (3.8-fold) compromised by PRDX4 shRNA. A less conspicuous (1.8-fold) impairment of collagen secretion was also noted in ERO1 wild-type PRDX4 shRNA cells (Figure 4B). Both the secretory defect and the hypersensitivity of cells with a combined deficiency of ERO1 and PRDX4 to DTT mirror the phenotype of yeast deficient in ERO1 (Frand and Kaiser, 1998) and suggest a defect in disulfide bond formation.

To directly assess the impact of PRDX4 knockdown on the reduction-oxidation (redox) equilibrium in the ER of ERO1 mutant

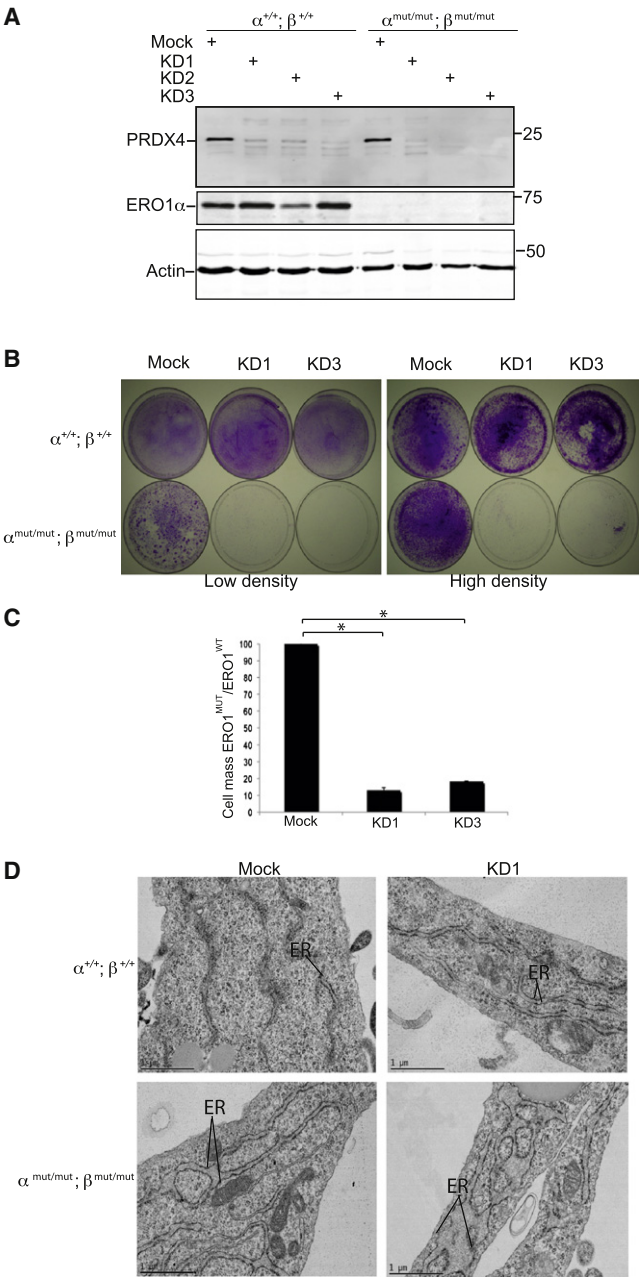

Figure 3. PRDX4 Buffers the Consequences of ERO1 Deficiency in MEFs

(A) Immunoblot of endogenous PRDX4, ERO1α, and actin in wild-type ($\alpha^{+/+};\beta^{+/+}$) and ERO1 mutant ($\alpha^{mut/mut};\beta^{mut/mut}$) MEFs 4 days after transduction with a *puro*^{r}-marked lentivirus carrying a irrelevant insert (mock) or three different short hairpin RNAs directed to mouse PRDX4.

(B) Crystal violet-stained plates following 2 weeks of puromycin selection after seeding with 8×10^3 (low density) or 4×10^4 (high density) MEFs of the indicated genotype and transduction with *puro*^{r}-tagged lentivirus carrying the indicated shRNA.

(C) Bar diagram of the ratio of cell mass accrued in the ERO1-double-mutant versus wild-type MEFs from the experiment shown in (B). The ratio was normalized to 1 in the cells transduced with the irrelevant shRNA. Shown are means ± SEM of a typical experiment reproduced three times (n = 3, *p < 0.05).

(D) Transmission electron micrographs of MEFs of the indicated genotype after transduction with a lentivirus containing an irrelevant shRNA or an shRNA directed to PRDX4. Note the dilation of the ER in the mutant cells transduced with the shRNA to PRDX4.

cells, we transduced cells with FLAG-M1-tagged, ER-localized reduction-oxidation sensitive green fluorescent protein (roGFP-iE). This altered version of the fluorescent protein is engineered to contain two exposed cysteines that form a relatively unstable disulfide with a redox potential of −235 ± 7 mV. roGFP-iE is thus suited to report on changes in the redox poise of oxidizing environments such as the ER (Lohman and Remington, 2008). The FLAG-M1-roGFP-iE immunopurified from the ER of cells with a combined deficiency of ERO1 and PRDX4 was predominantly reduced (89%), whereas that purified from the ER of cells with intact PRDX4 was a mixture of reduced (55%) and oxidized protein (44%) (Figures 4C and 4D). Because the FLAG-M1 antibody only detects FLAG-roGFP-iE after signal peptide cleavage, this assay is not influenced by variation in the efficiency with which the protein translocates into the ER, and our observations strongly support an oxidative defect in ERO1 mutant cells lacking PRDX4.

ER-Localized, Enzymatically Active PRDX4 Rescues a Lethal Mutation of Yeast ERO1

Yeast lack a known ER-localized peroxiredoxin. Therefore, we asked whether introducing mammalian PRDX4 into the yeast ER could rescue the lethal phenotype of a strong *ERO1* mutation. The FLAG-M1-tagged coding sequence of mature mouse PRDX4 was fused in frame to the cleavable yeast proalpha mating factor signal sequence, and the chimeric protein was expressed from the yeast CUP1 promoter as a plasmid episome. Upon transduction of this plasmid, haploid yeast with the highly penetrant temperature-sensitive *ero1-1* mutation (Frand and Kaiser, 1998) acquired the ability to grow at the nonpermissive temperature (Figure 5A). Expression of PRDX4 had no deleterious effect on growth at the permissive temperature, whereas the growth of the rescued *ero1-1* yeast at the nonpermissive temperature approached their growth rate at the permissive temperature (Figure 5B).

Basal activity of the *CUP1* promoter was sufficient; addition of copper did not enhance the rescue. To confirm that the robust rescue noted above was imparted by persistent expression of the PRDX4 plasmid, we exploited the fact that the *URA3*(+) auxotrophic marker can be used for both positive and negative selection for the presence of the plasmid. URA3-deficient parental and *ero1-1* yeast that had been transformed by the empty pRS316- or PRDX4-expressing plasmid were selected for presence of the plasmid in media lacking uracil at the permissive temperature. They were then spotted onto synthetic, minimal medium (SD) plates that either did or did not contain 5-fluoroorotic acid (FOA), which is converted to the toxin 5′ fluorouracil by orotidine-5′-phosphate decarboxylase (encoded by *URA3*). At the permissive temperature both the wild-type and the *ero1-1* mutant yeast rid themselves of the URA3$^+$ PRDX4 expression plasmid and survived the FOA selection. However, at the nonpermissive temperature only the wild-type yeast grew on

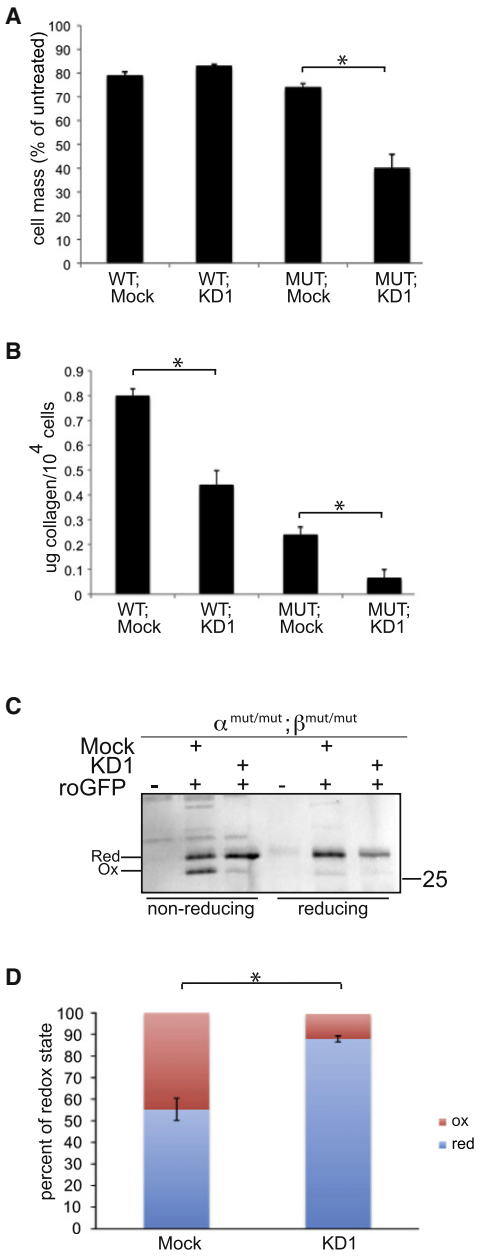

Figure 4. Hypersensitivity to Reducing Agents, Defective Collagen Secretion, and a More Reduced ER Redox Poise in ERO1-Deficient Cells Lacking PRDX4

(A) Bar diagram of cell mass of wild-type (WT) or *Ero1*$\alpha^{mut/mut}$;*Ero1*$\beta^{mut/mut}$ compound mutant cells (MUT) transduced with mock or PRDX4 RNAi lentivirus (KD1) remaining 3 hr after a 30 min pulse with DTT (5 mM) followed by recovery in normal media, normalized to the cell mass of a parallel culture of the same cells that had not been exposed to DTT. Shown are aggregate means ± SEM from a typical experiment conducted in triplicate (n = 3; *p < 0.05) and reproduced three times.

(B) Bar diagram of soluble collagen secreted into the conditioned media from the cells described in (A) normalized to the number of live cells in the culture. Shown are means ± SEM from three experiments conducted on different occasions in triplicate (n = 9; *p < 0.01).

(C) Immunoblot of FLAG-M1-roGFP-iE immunopurified from the ER of ERO1-deficient MEFs with normal levels of PRDX4 or PRDX4 knockdown. The purified proteins were resolved by SDS-PAGE under nonreducing or reducing conditions. The position of the reduced and oxidized FLAG-M1-roGFP-iE in a typical experiment reproduced three times is shown.

(D) Quantitative representation of the data from the experiment represented in (C). The bar diagram shows the ratio of reduced and oxidized roGFP in the *Ero1*$\alpha^{mut/mut}$;*Ero1*$\beta^{mut/mut}$ compound mutant cells transduced with mock or PRDX4 RNAi lentivirus (KD1) (n = 3, *p < 0.05, comparing oxidized fraction in the two genotypes).

FOA (Figure 5C). These findings indicate that rescue of *ero1-1* is due to persistent expression of the PRDX4- expression plasmid.

In addition to their thiol-mediated peroxidase activity, members of the peroxiredoxin family also have chaperone activity (Hall et al., 2009). To determine whether the rescue of the growth defect of *ero1-1* mutant is mediated by the peroxidase activity or by the chaperone activity, we mutated the two active-site cysteines of PRDX4 in the yeast expression plasmid. To test whether localization to the ER is required for rescue, we removed the signal sequence from the protein. All three mutants were well expressed in the *ero1-1* yeast, but only the ER-localized wild-type PRDX4 rescued the temperature-sensitive phenotype of the *ero1-1* mutant (Figure 5D).

We were unable to come to a firm conclusion in regard to the source of H_2O_2 driving oxidation of PRDX4 in yeast or in mammalian cells. Respiratory-deficient *ero1-1* yeast compromised by deletion of *coq3* were nonetheless rescued by PRDX4, indicating that an intact respiratory chain is not a requisite for PRDX4-mediated oxidation in yeast (Figure S1A, available online). Similarly, ERO1-deficient MEFs are not conspicuously hypersensitive to compromise of mitochondrial gene expression by culture in media containing ethidium bromide, nor are they hypersensitive to diphenylene iodonium (DPI), an inhibitor of NADPH oxidase (data not shown). Finally, this theme of redundancy in H_2O_2 source(s) is also reflected by the apparent lack of effect of ERO1 genotype on the rate of endogenous PRDX4 reoxidation after a pulse of DTT (Figure S1B).

PRDX4 Catalyzes H_2O_2 and PDI-Dependent Oxidative Refolding of RNase A In Vitro

Ruddock and colleagues have discovered that H_2O_2 can directly serve as an electron acceptor in PDI-mediated oxidative refolding of RNase A in vitro (Karala et al., 2009). The ability of PRDX4 to accelerate this thermodynamically favored process would serve as a strong test of the hypothesis that PRDX4 accelerates disulfide bond formation by converting hydroperoxides to disulfides in the ER lumen.

First we tested PDI's ability to be oxidized by PRDX4 in vitro. Bacterially expressed PDI (150 μM) was reduced by DTT, desalted by gel filtration, and reacted with bacterially expressed wild-type PRDX4 (5 μM) or the active-site mutants PRDX4^{C127S} and PRDX4^{C248S} in the absence or presence of an H_2O_2-generating system consisting of glucose (2.5 mM) and glucose oxidase (10 milliunits/ml) (Figure 6A). The time-dependent oxidation of free thiols was assessed by loss of their reactivity with the Ellman's reagent [5,5′-dithiobis(2-nitrobenzoate, DTNB)]. Oxidation was dependent on a source of H_2O_2 and was accelerated by wild-type PRDX4 but not by the two active-site mutants (Figure 6B). In the absence of PDI, PRDX4 was unable to oxidize

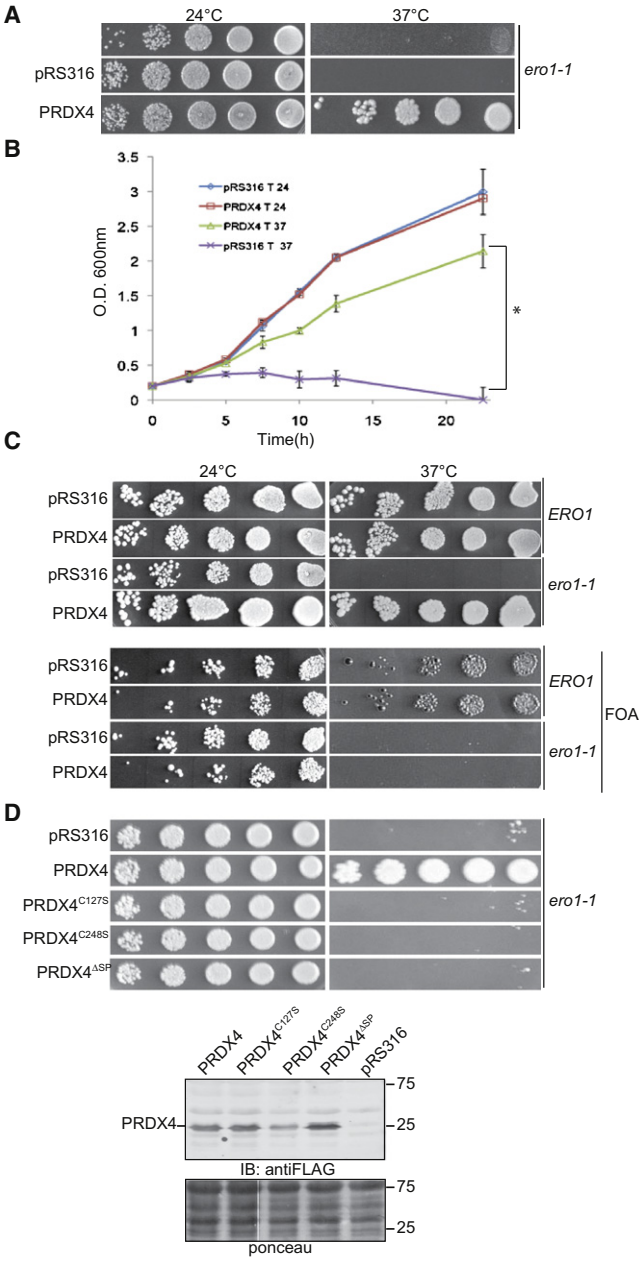

Figure 5. ER-Localized, Enzymatically Active PRDX4 Rescues a Lethal Mutation of Yeast ERO1

(A) Photomicrographs of serial dilutions of untransformed *ero1-1* mutant yeast or transformed with yeast expression plasmids lacking (pRS316) or containing the PRDX4 coding sequence cultured at the permissive temperature of 24°C or the nonpermissive temperature of 37°C.

(B) Plot of absorbance at 600 nm of cultures inoculated with *ero1-1* yeast transformed with the expression plasmids lacking (pRS316) or containing the PRDX4 coding sequence and cultured at the permissive temperature of 24°C or the nonpermissive temperature of 37°C. Shown are means ± SEM of a typical experiment conducted in triplicate (n = 3, *the last four time points, $p < 0.001$ by two-way ANOVA).

(C) Photomicrographs of serial dilutions of *ero1-1* yeast transformed with pRS316 or the PRDX4 expressing plasmids and plated in the absence or presence of the toxin FOA at 24°C or 37°C. Note the inability of the *ero1-1* yeast transformed with the PRDX4 expression plasmid to survive on FOA at the nonpermissive temperature.

(D) Photomicrographs of serial dilutions of *ero1-1* yeast transformed with pRS316 or plasmids expressing wild-type or the indicated mutations in PRDX4 (ΔSP: lacks the signal peptide required for ER import of PRDX4). The lower panel is an immunoblot of FLAG-tagged PRDX4 from the four transformed strains and the parental *ero1-1* yeast.

reduced glutathione, indicating selectivity for the source of electrons in this reaction (Figure 6C).

To determine whether the accelerated oxidation of PDI would give rise to accelerated oxidation of reduced and denatured RNase A, we monitored the latter's mobility on nonreduced SDS-PAGE at different time points in an in vitro refolding reaction. In reactions containing an H_2O_2-generating system with PRDX4 and PDI, the low-mobility, reduced RNase A forms were rapidly converted to high-mobility forms that comigrated with native RNase A. Omitting any of the three components markedly attenuated this conversion, and active-site mutants of PRDX4 were ineffective (Figure 6D). These observations indicate that efficient PRDX4-mediated oxidative folding of RNase A requires active peroxiredoxin, an electron acceptor (H_2O_2, in this case), and an oxidoreductase (PDI).

To determine whether the refolded RNase A was functional, or whether PRDX4-mediated refolding favored scrambled RNase A, we monitored RNase A enzymatic activity by using cyclic cytidine 5′-monophosphate (cCMP) as a substrate (Lyles and Gilbert, 1991). The time-dependent acquisition of RNase A activity correlated well with the rate of refolding on the SDS-PAGE, indicating that the disulfide bonds formed in the presence of PRDX4 and PDI are native (Figure 6E). Together these observations establish that PRDX4 possesses the enzymatic activity required to substitute for the lack of ERO1.

DISCUSSION

We have discovered that PRDX4 buffers the growth-inhibitory consequences of ERO1 deficiency in settings ranging from yeast to cultured mouse cells. Such buffering requires expression of PRDX4 in the lumen of the ER and is dependent on the two cysteines of PRDX4 that are involved in its peroxidase activity. In vitro, PRDX4 is able to accelerate the H_2O_2-dependent oxidative folding of reduced and denatured RNase A in the presence of PDI. Together, these observations point to an unanticipated role for PRDX4 in converting ER lumenal H_2O_2 to disulfides and in handing these disulfides over to PDI for oxidation of newly synthesized secretory proteins (Figure 7).

Neither yeasts nor worms, species in which ERO1 is essential (Frand and Kaiser, 1998; Pollard et al., 1998), have genes encoding predicted ER-localized peroxiredoxins, whereas more complex eukaryotes, such as flies and mice, in which ERO1 is not essential to cell viability, have PRDX4 genes. This correlation, together with the relatively broad expression of PRDX4 in mouse tissues (Iuchi et al., 2009) and the ability of PRDX4 to rescue ERO1 deficiency in the heterologous yeast system, suggests that PRDX4 may be broadly implicated in the observed redundancy of ERO1 in higher eukaryotes.

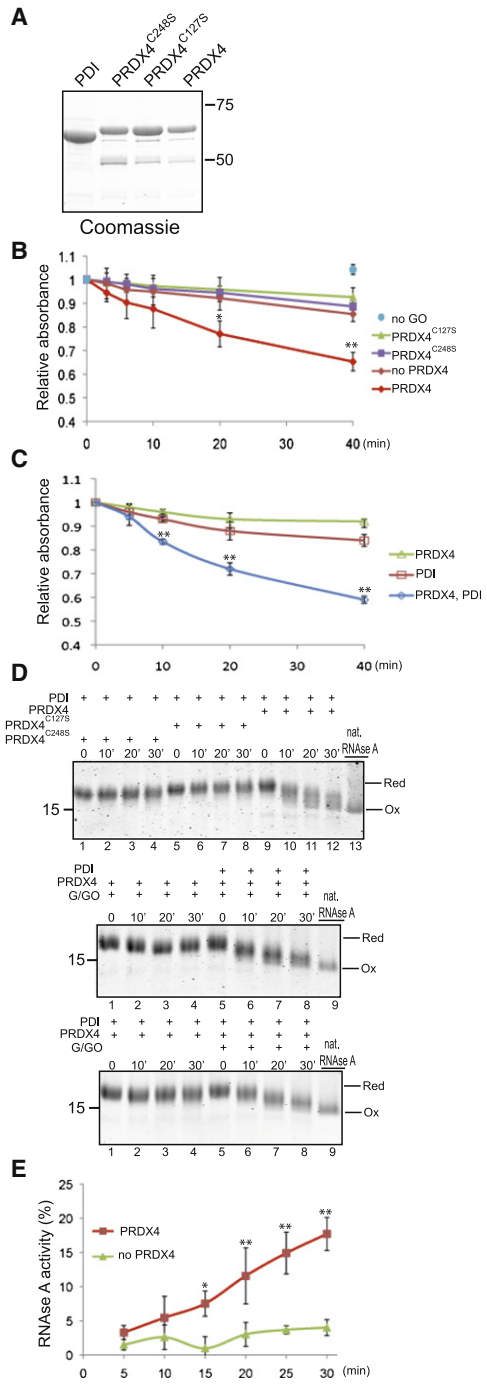

Figure 6. PRDX4 Catalyzes H_2O_2- and PDI-Dependent Oxidative Refolding of RNase A In Vitro

(A) Coomassie-stained reducing SDS-PAGE of purified PDI, wild-type, and mutant PRDX4-GST tagged proteins used in the experiments shown below.

(B) Time-dependent change in absorbance of Ellman's reagent reacted with reduced PDI (150 μM) after introduction of glucose (2.5 mM) and glucose oxidase (GO, 10 mU/ml) as a source of H_2O_2 and the indicated wild-type or mutant PRDX4 proteins shown in (A) (5 μM). The absorbance of each reaction mixture at t = 0 is set at 100%. Shown are means ± SEM of a typical assay conducted in triplicate and reproduced four times (n = 3, *p < 0.05, **p < 0.001).

Peroxiredoxins are pentamers of homodimers. Their catalytic mechanism entails a nucleophilic attack by a peroxidic cysteine (C127, in mouse PRDX4) on a hydroperoxide (probably H_2O_2), leading to the formation of a sulfenic acid intermediate that is resolved by a second active-site cysteine (C248) from an adjoining protomer. The resulting intersubunit disulfide is later reduced by a thioredoxin-like protein, completing the catalytic cycle (Hall et al., 2009). Our in vitro studies and the crystal structure of human PRDX4 in the reduced state (PDB: 2PN8) are both consistent with this catalytic mechanism and indicate that unlike ERO1, PRDX4 cannot utilize molecular oxygen as the electron acceptor and must instead rely on a source of hydroperoxides.

ERO1 generates one molecule of H_2O_2 for every disulfide bond formed (Gross et al., 2006). Recent measurements suggest that despite being a nonpolar molecule and thus freely diffusible across membranes, H_2O_2 produced in the ER by ERO1 activity is consumed in that compartment (Enyedi et al., 2010). PRDX4 would be well positioned to use that peroxide to generate another pair of disulfides, enhancing the efficiency of oxidative protein folding (Figure 7). Such an arrangement would have the additional benefit of reducing reactive H_2O_2 to water, as suggested by Bulleid and colleagues (Tavender and Bulleid, 2010). In this vein, it is interesting to note that in worms and yeast, which lack a PRDX4-mediated pathway to eliminate ERO1-generated H_2O_2, attenuation of ERO1 activity provides some protection against the lethality of severe unfolded protein stress in the ER (Haynes et al., 2004; Marciniak et al., 2004). However, no such benefit was observed in the insulin-producing β cells of the mouse pancreas, which have ample PRDX4 (Zito et al., 2010, and unpublished data). This suggests that the high levels of PRDX4 in the pancreas (Iuchi et al., 2009) and β cells efficiently scavenge and utilize the H_2O_2 produced by ERO1.

Clearly a different source of H_2O_2 is driving PRDX4-dependent disulfide bond formation in cells lacking ERO1. Mitochondria are candidates, and their involvement may explain previous reports of mitochondrial respiration-dependent production of disulfides in mammalian cells (Yang et al., 2007). Junctions known to exist between mitochondria and ER membranes (Kornmann et al., 2009) could serve to channel H_2O_2 into the ER (and away from

(C) Time-dependent change in absorbance of Ellman's reagent in reaction mixes containing 150 μM reduced glutathione in the presence of PDI (10 μM), PRDX4 (5 μM), or both enzymes. Glucose (2.5 mM) and glucose oxidase (GO, 10 mU/ml) were included as a source of H_2O_2 in all reactions. The absorbance of each reaction mixture at t = 0 is set at 100%. Shown are means ± SEM of a typical assay conducted in triplicate and reproduced three times (n = 3, **p < 0.001).

(D) Coomassie-stained SDS-PAGE of reduced and denatured RNase A (25 μM) after reacting for the indicated time with reduced PDI (7 μM) and PRDX4 (5 μM) in the presence of glucose (2.5 mM) and glucose oxidase (10 mU/ml) as a source of H_2O_2. Lane 13 in the top panel or lane 9 in the two lower panels contains a sample of native oxidized RNase A to serve as a reference.

(E) Time-dependent change in RNase activity measured spectrophotometrically by absorbance at 296 nm with cCMP (4.5 mM) as substrate. The refolding of RNase A was initiated at t = 0 in reactions as in (D). Enzymatic activity of an equal amount of native RNase A is set as 100%. Shown are means ± SEM of a typical experiment reproduced four times (n = 3, *p < 0.05, **p < 0.001 by two-way ANOVA).

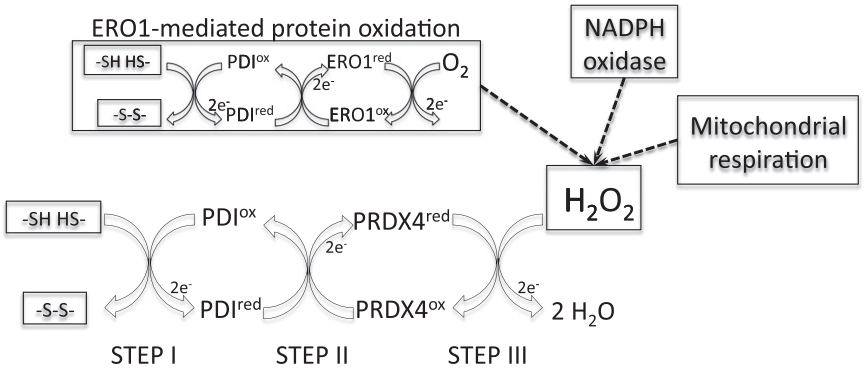

Figure 7. Model for PRDX4-Mediated Oxidative Protein Folding in the ER

Disulfide bond formation (step I) leaves PDI in a reduced state. PDI is reoxidized by reducing the active-site disulfide (formed between two PRDX4 protomers) in step II. PRDX4 is reoxidized by interaction of its peroxidic cysteine (C127) with H_2O_2, releasing one molecule of water. The sulfenic acid is resolved by C287, regenerating the disulfide and releasing the second molecule of water (step III). PRDX4 may utilize H_2O_2 produced by ERO1 as well as H_2O_2 produced by mitochondrial respiration or NADPH oxidases.

cytosolic peroxiredoxins) to be used for PRDX4-mediated oxidative protein folding (Figure 7).

In β cells, the tight coupling of mitochondrial respiration to nutrient availability may provide a mechanism for accelerated disulfide bond formation during proinsulin synthesis, as the latter is translationally activated by nutrients (Itoh and Okamoto, 1980). Such an arrangement may also clarify an interesting peculiarity of β cells in that they contain superoxide dismutases (that convert oxygen radicals to H_2O_2) but lack glutathione peroxidase or catalase activity to break down H_2O_2 (Tiedge et al., 1997). This feature may have evolved to enable β cells to efficiently harness H_2O_2 for disulfide bond formation required during proinsulin folding.

H_2O_2 may also be produced by NADPH oxidases. The latter are integral membrane proteins activated posttranslationally by a variety of signals, including growth factor receptors (Goldstein et al., 2005). Cytosolic peroxiredoxins channel the H_2O_2 produced by NADPH oxidases to regulate the activity of signaling molecules such as oxidation-sensitive phosphatases (Woo et al., 2010). It is tempting to speculate that a conceptually similar diffusion of H_2O_2 into the ER from ER-localized NADPH oxidases may couple extracellular signaling to ER protein oxidation.

Two-cysteine peroxiredoxins are subject to inactivation by formation of a sulfinic acid on the peroxidic cysteine. In the cytosol this reaction is reversed by a sulfiredoxin that reduces the sulfenic acid in an ATP-dependent reaction (Biteau et al., 2003). There are no known sulfiredoxins in the ER, suggesting that inactivation of PRDX4 by formation of a cysteine-sulfinic acid might be irreversible (Tavender and Bulleid, 2010). Such irreversible inactivation of PRDX4 by excess H_2O_2 may account for the seemingly paradoxical induction of unfolded protein stress in the ER under hyperoxidizing conditions and its relief by antioxidants (Malhotra et al., 2008). Alternatively, inactivation of PRDX4 by elevated levels of H_2O_2 may regulate the disulfide-based redox poise of the ER, akin to the allosteric inhibition of ERO1 by oxidized PDI (Sevier et al., 2007).

Our discovery of a PRDX4-dependent pathway operating in parallel to ERO1-mediated protein oxidation in the ER does not preclude the existence of other parallel pathways that might be revealed by the phenotype of compound ERO1 and PRDX4 deficiency in other systems. Regardless of whether further redundancy exists, this study points to an unanticipated level of complexity of oxidative protein folding in higher eukaryotes and suggests a mechanism for regulating this conserved process by the availability of H_2O_2.

EXPERIMENTAL PROCEDURES

Isolation, Culture, and Metabolic Labeling of LPS Blasts

Splenic cells from wild-type and compound homozygous *Ero1α;Ero1β* mutant mice (Zito et al., 2010) were cultured in RPMI-1640 at a density of 10^6 cells/ml and exposed to 50 μg/ml lipopolysaccaride from *Escherichia coli* (Sigma, L2755) for 2–3 days. After a 15 min labeling pulse with 60 μCi/ml of [^{35}S]methionine/cysteine (Perkin Elmer; specific activity, > 1,000 Ci/mmol), a cold chase was performed in complete media followed by lysis and immunopurification of the radiolabeled IgM with 5 μl of rabbit anti-mouse IgM (Rockland). Immunoprecipitated proteins were resolved on reducing and nonreducing 10% SDS-PAGE and revealed by autoradiography with a Typhoon Phosphoimager (GE Healthcare).

Immunopurification of Complexes Trapped by FLAG-PDI

Expression plasmids encoding ER-localized, N-terminally FLAG-tagged human PDI (PDIA1, 18–508) were constructed in the pFLAG-CMV1 vector (Sigma). The C-terminal FLAG-PDI^{C400S} and double-trapping mutant FLAG-PDI$^{C56S;C400S}$ were made by QuikChange Site-Directed Mutagenesis (Stratagene). Transfected HEK293T cells from four confluent 100 mm plates were washed in phosphate-buffered saline (PBS) with 20 mM NEM and lysed in 0.3% Triton X-100, 150 mM NaCl, 20 mM HEPES (pH 7.4), 10 mM CaCl2, 20 mM NEM, and protease inhibitors. The FLAG-tagged proteins were immunopurified with FLAG-M1 affinity gel (Sigma) in an overnight incubation and eluted in 10 mM EDTA, 20 mM Tris (pH 7.5), and 0.002% Tween 20. Ten percent of the eluted material was immunoblotted with anti-FLAG M2 (Sigma), rabbit anti-ERO1α antiserum (Zito et al., 2010), or rabbit anti PRDX4 (a gift of Junichi Fujii) (Matsumoto et al., 1999) after reducing and nonreducing SDS-PAGE. The residual 90% was resolved on nonreducing SDS-PAGE stained lightly with Coomassie, and the region of the gel containing complexes larger than the FLAG-PDI^{C400S} bait was excised, reduced in 10 mM DTT, alkylated with 20 mM NEM, and analyzed by mass spectrometry.

Mass Spectrometry

A linear ion trap (LTQ)-Orbitrap (ThermoFisher, Bremen, Germany) equipped with a nano-ESI source was used for all analyses. Samples were directly infused via a Eksigent 2DLC system (Eksigent Technologies, Dublin, CA) equipped with a 12 cm PicoFrit self-packed-column PicoTip emitter (75 μm ID, 10 μm tip diameter from New Objective, Woburn, MA) packed in house with ReproSil-Pur C18-AQ beads (3 μm from Dr. Maisch GmbH, Ammerbuch, Germany). Samples were applied with direct loading onto the analytical column (0.8 μl/ min for 25 min with mobile phase A; 0.1% formic acid). The flow rate was then changed to 0.3 μl/min and peptides were eluted with a gradient of 1%–76% acetonitrile in 0.1% formic acid over 120 min. Mass spectra were acquired in data-dependent mode with one 60,000 resolution MS survey

scan in the Orbitrap, followed by up to nine subsequent MS/MS scans in the LTQ from the nine most intense peaks detected in the survey scan. MS survey scans were acquired in profile mode and the MS/MS scans were acquired in centroid mode.

Generic MASCOT format files were generated from raw data with DTA SuperCharge (version 2.0a7) and searched by using MASCOT software (version 2.3, Matrix Science, London, UK). The human IPI database was searched with peptide mass tolerance of 20 ppm and fragment mass tolerance of 0.6 Da. Trypsin specificity was set to a maximum of one missed cleavage and NEM, NEM + water, and oxidation were set as variable modifications.

Lentiviral Transduction and Analysis of Wild-type and *Ero1α;Ero1β* Mutant MEFs

Wild-type and compound homozygous *Ero1α;Ero1β* mutant MEFs, isolated at embryonic day 13.5, were immortalized with SV-40 large T antigen and cultured in DMEM supplemented with 25 mM glucose, 10% FCS, and nonessential amino acids. *Prdx4* knockdown was achieved by using Mission shRNA-encoding lentiviruses directed to mouse *Prdx4* mRNA (Sigma SHCLNG-NM_016764) following the manufacturer's instructions. Knockdown clone KD1 was targeted with shRNA TRCN0000055339, KD2 with TRCN0000055341, and KD3 TRCN0000055339. After transduction and selection with puromycin at 4 μg/ml for 2 weeks, the cells (in triplicate plates) were fixed, stained with crystal violet, and photographed. KD2 had off-pathway toxicity and was not used in the phenotypic analysis. Cell mass was quantified by solubilizing the dye in 0.2% Triton X-100 and measuring the absorbance at 590 nm.

To assess the extent of knockdown achieved, we transduced 5×10^6 cells, selected them for 4 days with puromycin (a period sufficient to kill more than 95% of the nontransduced cells), and immunoblotted the cell lysate for PRDX4.

Secretion of soluble collagen was measured in the 24 hr conditioned media of MEFs by using the Sircol colorimetric assay (Biocolor, Ireland) according to the manufacturer's instruction. MEFs were cultured in media with 10% FCS for 48 hr before the assay and switched to media with 0.5% FCS to collect the conditioned media. The sensitivity of cells to reductive stress was measured by crystal violet staining of the cell mass that remained on the plate 3 hr after a 30 min challenge with 5 mM DTT.

The roGFP-iE cDNA (Lohman and Remington, 2008) was ligated in frame with the FLAG-M1 tag in a lentiviral vector to transduce cells of the indicated genotype. Cells were lysed in the presence of 20 mM NEM, and the FLAG-M1-roGFP-iE was immunoprecipitated with the FLAG-M1 monoclonal antibody, resolved on 15% SDS-PAGE in the absence or presence of DTT, and blotted with FLAG M2.

Cell pellets were fixed by immersion in 2% glutaraldehyde and 2.0% paraformaldehyde in 0.1 M sodium cacodylate buffer (pH 7.2), postfixed in 1% osmium tetroxide, and en bloc-stained with 1% uranyl acetate. The sample was dehydrated in ethanol embedded in Epon (Electron Microscopy Sciences, Hatfield, PA). Ultrathin sections were poststained with uranyl acetate and lead citrate and examined with an electron microscope (CM12, FEI, Eindhoven, The Netherlands) at 120 kV. Images were recorded digitally with a camera system (Gatan, 4k × 2.7k) with Gatan DigitalMicrograph software (Gatan Inc., Pleasanton, CA).

Yeast Strains and Plasmids

The temperature-sensitive yeast strain CKY598 bearing the *ero1-1* mutation (C. Kaiser Lab at MIT) and the wild-type strain were transformed with PRDX4-pRS316, in which the cleavable yeast α-mating-factor signal sequence is fused in frame with FLAG-M1-tagged mature wild-type or active-site mutant mouse PRDX4 (37–274) and expression driven by the yeast *CUP1* promoter and termination sequences from the *CPY1* gene. A cytosolic version was made by replacing the yeast α−mating factor signal sequence with an initiator methionine (yielding a protein nearly identical in size to mature ER version). Transformed yeast were selected on minimal media lacking uracil or SD media with and without 0.1% FOA (Sigma) and incubated at the permissive (24°C) or nonpermissive temperature (37°C).

Protein Oxidation In Vitro

Mouse $PRDX4^{WT}$ and the mutants $PRDX4^{C127S}$ and $PRDX4^{C248S}$ were expressed as glutathione S-transferase (GST) fusion proteins in *E. coli* Rosetta (D3) strain followed by glutathione affinity chromatography and gel filtration on Superdex 200. Human PDI (PDIA1 18-508), a gift of C. Thorpe, University of Delaware, was expressed in *E. coli* BL21 (D3) strain, purified with Ni-NTA affinity chromatography, and dialyzed into the reaction buffer.

PDI was reduced by incubation with 50 mM of DTT, 1 hr at room temperature, and then desalted on PD-10 gel filtration column (GE Healthcare). Oxidation in vitro was performed in the presence of glucose (2.5 mM) and glucose oxidase (10 mu/ml) type II from *Aspergillus niger* (Sigma) in 80 mM sodium phosphate, pH = 7.0. Where indicated reduced glutathione was added to the reaction. Free thiols were quantified at different time points by combining 100 μl of 0.5 mM Ellman's reagent [(5,5′-dithiobis-(2-nitrobenzoic acid)] with 30 μl of sample and absorbance at 405 nm measured in a Tecan Infinite 500 plate reader. In some assays reduced glutathione was added as an upstream electron donor.

RNase A (from bovine pancreas, Roche) was reduced and denaturated overnight in the presence of 6 M guanidinium hydrochloride and 140 mM DTT in 50 mM phosphate buffer, pH 7, and desalted into the assay buffer on PD-10 column before the refolding assays were run. Reduced RNase A (25 μM) was then incubated with PDI (7 μM) and PRDX4 (5 μM) in the presence of glucose (2.5 mM) and glucose oxidase (10 mu/ml) in 80 mM phosphate buffer, pH 7. Aliquots of 20 μl were withdrawn at different time points and reacted with 2 μl of 0.5 M NEM (NEM) for 15 min on ice. Refolding of RNaseA was then analyzed on an 18% Tris-tricine gel under nonreducing conditions.

The functional state of RNase A was measured by adding cytidine 2′,3′ cyclic monophosphate monosodium salt (cCMP from Sigma) and reading the development of absorbance from its hydrolytic product at 296 nm, in a temperature-controlled Agilent diode array spectrophotometer at 25°C, as described (Lyles and Gilbert, 1991).

Statistical Analysis

All results are expressed as means ± SEM. Two-tailed Student's t tests were performed to determine p values for paired samples, and two-way analysis of variance (ANOVA) was performed for the experiments that employed more than one independent variable.

SUPPLEMENTAL INFORMATION

Supplemental information includes one figure and can be found with this article online at doi:10.1016/j.molcel.2010.11.010.

ACKNOWLEDGMENTS

We thank C. Sevier and C. Kaiser (Massachusetts Institute of Technology) for the CKY598 *ero1-1* mutant yeast and advice on its use, A. Liang and E. Roth from the imaging core facility of NYU School of Medicine for processing and acquiring the EM images, J. Fujii (Yamagata University) for the antiserum to PRDX4, C. Thorpe (University of Delaware) for the gift of the PDI expression plasmid, J. Remington (University of Oregon) for the roGFP-iE, A. Tzagaloff (Columbia University) for the *coq3* deleted yeast and advice on its use, M. Costanzo (University of Toronto) for the *sec72Δ;ero1-1* compound haploid, and H. Klein and A. Epshtein (NYU) for advice and help with yeast genetics. This work was supported by an EMBO long-term fellowship ALTF649-2008 to E.Z., Fundação para a Ciência e Tecnologia, Portugal (SFRH/BSAB/922/2009, PTDC/QUI/73027/2006 and IBB/CBME LA) to E.P.M., by NIH grants DK47119, DK075311, and ES08681 to D.R. and NS050276, CA016087, and a grant from the 100 Women In Hedge Funds Foundation to T.A.N. D.R. is a Wellcome Trust Principal Research Fellow.

Received: June 17, 2010
Revised: August 11, 2010
Accepted: September 13, 2010
Published: December 9, 2010

REFERENCES

Appenzeller-Herzog, C., Riemer, J., Christensen, B., Sørensen, E.S., and Ellgaard, L. (2008). A novel disulphide switch mechanism in Ero1alpha balances ER oxidation in human cells. EMBO J. *27*, 2977–2987.

Baker, K.M., Chakravarthi, S., Langton, K.P., Sheppard, A.M., Lu, H., and Bulleid, N.J. (2008). Low reduction potential of Ero1alpha regulatory disulphides ensures tight control of substrate oxidation. EMBO J. *27*, 2988–2997.

Biteau, B., Labarre, J., and Toledano, M.B. (2003). ATP-dependent reduction of cysteine-sulphinic acid by S. cerevisiae sulphiredoxin. Nature *425*, 980–984.

Blais, J.D., Chin, K.T., Zito, E., Zhang, Y., Heldman, N., Harding, H.P., Fass, D., Thorpe, C., and Ron, D. (2010). A small molecule inhibitor of endoplasmic reticulum oxidation 1 (ERO1) with selectively reversible thiol reactivity. J. Biol. Chem. *285*, 20993–21003.

Brizzard, B.L., Chubet, R.G., and Vizard, D.L. (1994). Immunoaffinity purification of FLAG epitope-tagged bacterial alkaline phosphatase using a novel monoclonal antibody and peptide elution. Biotechniques *16*, 730–735.

Cabibbo, A., Pagani, M., Fabbri, M., Rocchi, M., Farmery, M.R., Bulleid, N.J., and Sitia, R. (2000). ERO1-L, a human protein that favors disulfide bond formation in the endoplasmic reticulum. J. Biol. Chem. *275*, 4827–4833.

Dias-Gunasekara, S., Gubbens, J., van Lith, M., Dunne, C., Williams, J.A., Kataky, R., Scoones, D., Lapthorn, A., Bulleid, N.J., and Benham, A.M. (2005). Tissue-specific expression and dimerization of the endoplasmic reticulum oxidoreductase Ero1beta. J. Biol. Chem. *280*, 33066–33075.

Enyedi, B., Várnai, P., and Geiszt, M. (2010). Redox state of the endoplasmic reticulum is controlled by Ero1L-alpha and intraluminal calcium. Antioxid. Redox Signal. *13*, 721–729.

Frand, A.R., and Kaiser, C.A. (1998). The ERO1 gene of yeast is required for oxidation of protein dithiols in the endoplasmic reticulum. Mol. Cell *1*, 161–170.

Goldstein, B.J., Mahadev, K., Wu, X., Zhu, L., and Motoshima, H. (2005). Role of insulin-induced reactive oxygen species in the insulin signaling pathway. Antioxid. Redox Signal. *7*, 1021–1031.

Gross, E., Sevier, C.S., Heldman, N., Vitu, E., Bentzur, M., Kaiser, C.A., Thorpe, C., and Fass, D. (2006). Generating disulfides enzymatically: reaction products and electron acceptors of the endoplasmic reticulum thiol oxidase Ero1p. Proc. Natl. Acad. Sci. USA *103*, 299–304.

Hall, A., Karplus, P.A., and Poole, L.B. (2009). Typical 2-Cys peroxiredoxins—structures, mechanisms and functions. FEBS J. *276*, 2469–2477.

Haynes, C.M., Titus, E.A., and Cooper, A.A. (2004). Degradation of misfolded proteins prevents ER-derived oxidative stress and cell death. Mol. Cell *15*, 767–776.

Hwang, C., Sinskey, A.J., and Lodish, H.F. (1992). Oxidized redox state of glutathione in the endoplasmic reticulum. Science *257*, 1496–1502.

Ikeda, Y., Ito, R., Ihara, H., Okada, T., and Fujii, J. (2010). Expression of N-terminally truncated forms of rat peroxiredoxin-4 in insect cells. Protein Expr. Purif. *72*, 1–7.

Ishihama, Y., Oda, Y., Tabata, T., Sato, T., Nagasu, T., Rappsilber, J., and Mann, M. (2005). Exponentially modified protein abundance index (emPAI) for estimation of absolute protein amount in proteomics by the number of sequenced peptides per protein. Mol. Cell. Proteomics *4*, 1265–1272.

Itoh, N., and Okamoto, H. (1980). Translational control of proinsulin synthesis by glucose. Nature *283*, 100–102.

Iuchi, Y., Okada, F., Tsunoda, S., Kibe, N., Shirasawa, N., Ikawa, M., Okabe, M., Ikeda, Y., and Fujii, J. (2009). Peroxiredoxin 4 knockout results in elevated spermatogenic cell death via oxidative stress. Biochem. J. *419*, 149–158.

Karala, A.R., Lappi, A.K., Saaranen, M.J., and Ruddock, L.W. (2009). Efficient peroxide-mediated oxidative refolding of a protein at physiological pH and implications for oxidative folding in the endoplasmic reticulum. Antioxid. Redox Signal. *11*, 963–970.

Kodali, V.K., and Thorpe, C. (2010). Oxidative protein folding and the quiescin-sulfhydryl oxidase family of flavoproteins. Antioxid. Redox. Signal. *13*, 1217–1230.

Kornmann, B., Currie, E., Collins, S.R., Schuldiner, M., Nunnari, J., Weissman, J.S., and Walter, P. (2009). An ER-mitochondria tethering complex revealed by a synthetic biology screen. Science *325*, 477–481.

Li, W., Schulman, S., Dutton, R.J., Boyd, D., Beckwith, J., and Rapoport, T.A. (2010). Structure of a bacterial homologue of vitamin K epoxide reductase. Nature *463*, 507–512.

Liu, M., Hodish, I., Rhodes, C.J., and Arvan, P. (2007). Proinsulin maturation, misfolding, and proteotoxicity. Proc. Natl. Acad. Sci. USA *104*, 15841–15846.

Lohman, J.R., and Remington, S.J. (2008). Development of a family of redox-sensitive green fluorescent protein indicators for use in relatively oxidizing subcellular environments. Biochemistry *47*, 8678–8688.

Lyles, M.M., and Gilbert, H.F. (1991). Catalysis of the oxidative folding of ribonuclease A by protein disulfide isomerase: pre-steady-state kinetics and the utilization of the oxidizing equivalents of the isomerase. Biochemistry *30*, 619–625.

Malhotra, J.D., Miao, H., Zhang, K., Wolfson, A., Pennathur, S., Pipe, S.W., and Kaufman, R.J. (2008). Antioxidants reduce endoplasmic reticulum stress and improve protein secretion. Proc. Natl. Acad. Sci. USA *105*, 18525–18530.

Marciniak, S.J., Yun, C.Y., Oyadomari, S., Novoa, I., Zhang, Y., Jungreis, R., Nagata, K., Harding, H.P., and Ron, D. (2004). CHOP induces death by promoting protein synthesis and oxidation in the stressed endoplasmic reticulum. Genes Dev. *18*, 3066–3077.

Matsumoto, A., Okado, A., Fujii, T., Fujii, J., Egashira, M., Niikawa, N., and Taniguchi, N. (1999). Cloning of the peroxiredoxin gene family in rats and characterization of the fourth member. FEBS Lett. *443*, 246–250.

Mezghrani, A., Fassio, A., Benham, A., Simmen, T., Braakman, I., and Sitia, R. (2001). Manipulation of oxidative protein folding and PDI redox state in mammalian cells. EMBO J. *20*, 6288–6296.

Pagani, M., Fabbri, M., Benedetti, C., Fassio, A., Pilati, S., Bulleid, N.J., Cabibbo, A., and Sitia, R. (2000). Endoplasmic reticulum oxidoreductin 1-lbeta (ERO1-Lbeta), a human gene induced in the course of the unfolded protein response. J. Biol. Chem. *275*, 23685–23692.

Pollard, M.G., Travers, K.J., and Weissman, J.S. (1998). Ero1p: a novel and ubiquitous protein with an essential role in oxidative protein folding in the endoplasmic reticulum. Mol. Cell *1*, 171–182.

Saaranen, M.J., Karala, A.R., Lappi, A.K., and Ruddock, L.W. (2010). The role of dehydroascorbate in disulfide bond formation. Antioxid. Redox Signal. *12*, 15–25.

Sevier, C.S., and Kaiser, C.A. (2008). Ero1 and redox homeostasis in the endoplasmic reticulum. Biochim. Biophys. Acta *1783*, 549–556.

Sevier, C.S., Qu, H., Heldman, N., Gross, E., Fass, D., and Kaiser, C.A. (2007). Modulation of cellular disulfide-bond formation and the ER redox environment by feedback regulation of Ero1. Cell *129*, 333–344.

Tavender, T.J., and Bulleid, N.J. (2010). Peroxiredoxin IV protects cells from oxidative stress by removing H2O2 produced during disulphide formation. J. Cell Sci. *123*, 2672–2679.

Tavender, T.J., Sheppard, A.M., and Bulleid, N.J. (2008). Peroxiredoxin IV is an endoplasmic reticulum-localized enzyme forming oligomeric complexes in human cells. Biochem. J. *411*, 191–199.

Tiedge, M., Lortz, S., Drinkgern, J., and Lenzen, S. (1997). Relation between antioxidant enzyme gene expression and antioxidative defense status of insulin-producing cells. Diabetes *46*, 1733–1742.

Tien, A.C., Rajan, A., Schulze, K.L., Ryoo, H.D., Acar, M., Steller, H., and Bellen, H.J. (2008). Ero1L, a thiol oxidase, is required for Notch signaling through cysteine bridge formation of the Lin12-Notch repeats in Drosophila melanogaster. J. Cell Biol. *182*, 1113–1125.

Tsai, B., and Rapoport, T.A. (2002). Unfolded cholera toxin is transferred to the ER membrane and released from protein disulfide isomerase upon oxidation by Ero1. J. Cell Biol. *159*, 207–216.

Tu, B.P., and Weissman, J.S. (2004). Oxidative protein folding in eukaryotes: mechanisms and consequences. J. Cell Biol. *164*, 341–346.

Wang, L., Li, S.J., Sidhu, A., Zhu, L., Liang, Y., Freedman, R.B., and Wang, C.C. (2009). Reconstitution of human Ero1-Lalpha/protein-disulfide isomerase oxidative folding pathway in vitro. Position-dependent differences in role between the a and a' domains of protein-disulfide isomerase. J. Biol. Chem. *284*, 199–206.

Woo, H.A., Yim, S.H., Shin, D.H., Kang, D., Yu, D.Y., and Rhee, S.G. (2010). Inactivation of peroxiredoxin I by phosphorylation allows localized H(2)O(2) accumulation for cell signaling. Cell *140*, 517–528.

Yang, Y., Song, Y., and Loscalzo, J. (2007). Regulation of the protein disulfide proteome by mitochondria in mammalian cells. Proc. Natl. Acad. Sci. USA *104*, 10813–10817.

Zito, E., Chin, K.T., Blais, J., Harding, H.P., and Ron, D. (2010). ERO1-β, a pancreas-specific disulfide oxidase, promotes insulin biogenesis and glucose homeostasis. J. Cell Biol. *188*, 821–832.